An Integrated Energy Demand Response Model Considering Source-Load Synergy and Stepped Carbon Trading Mechanism

Yi Zhang, Lin Li*, Wei Hu

Abstract—**Aiming at the problems of poor scheduling flexibility and insufficient carbon emission reduction capacity of the current integrated energy system, this paper proposes an optimization scheduling model of integrated energy demand response that combines source-load synergy with reward and punishment stepped carbon trading mechanism. Firstly, the integrated energy system operation architecture including electricity-heat-cooling energy was constructed to harmonize the energy generation side and consumption side and effectively improve the multi-energy complementary capability of the system. Secondly, the reward and punishment stepped carbon trading mechanism is established by combining the initial carbon quota allocation method and the actual carbon emission calculation theory, so that environmental friendliness and economic sustainability are effectively improved. Finally, to minimize the system operating cost, an integrated demand response optimal dispatch model that considers the characteristics of electric, thermal and cooling loads is constructed to determine the optimal dispatch scheme for the integrated energy system. The results of the calculation example indicate that the proposed integrated demand response model has the function of peak reduction and valley correction, energy conservation and carbon reduction, and provides a feasible solution for the integrated energy system optimal scheduling.**

Index Terms—**integrated demand response, integrated energy system, load optimization scheduling, stepped carbon trading, renewable energy**

I. Introduction

Recently, the problem of energy shortage and ecological deterioration in China has become increasingly severe, and the search for a clean, economic and efficient energy market model has received widespread attention [1]-[2]. However, the natural fluctuation and unpredictability of renewable energy significantly limit its capacity to be utilized on a widespread level, presenting a significant obstacle to the consistent and dependable supply of energy [3]-[4]. To enhance the utilization of renewable energy and decrease the environmental load, an integrated energy system (IES) that incorporates several energy sources has been actively pushed and implemented to optimize energy scheduling [5]. Within the integrated energy system, energy equipment makes all kinds of energy transform each other in the process of energy transportation and distribution, and improves the integration degree and conversion efficiency of energy [6]. Nevertheless, as electricity market reform progresses, customers are demanding increased levels of security and dependability in energy use [7]-[8]. Hence, how to tap the potential of integrated energy systems for integrated energy demand response is significantly important in promoting the green transition and ensuring sustainable growth of the economy and society.

Demand response (DR) is a crucial method of managing the demand side of energy use. End users autonomously adjust their energy consumption based on time-sharing tariffs and grid directives to meet the objectives of reducing peak demand and filling low-demand periods, as well as adjusting load peaks [9]. The problem of optimal scheduling of loads considering demand response has been extensively studied. For example, Nnamdi et al. [10] thoroughly examined the incentive demand response mode in microgrid operation. They achieved the optimal dispatch plan by minimizing the cost of power generation fuel and transferable load, while maximizing the demand response benefits for the microgrid operator. Yang et al. [11] studied the most effective approach for demand response and conducted a reliability analysis using time-sharing pricing and CPR strategy. They presented a model that divides the time into peak, valley, and regular periods based on the Fuzzy clustering technique. This model enhances the economic efficiency and reliability of power generation. Ming et al. [12] demonstrate that an incentive-based de-mand response program combining dynamic coupons and periodic lotteries can substantially reduce demand response costs while achieving a reasonable level of demand reduction. Lu et al. [13] proposed an AI-based demand response method for grid incentives, which relies on artificial intelligence. The researchers utilized deep neural network models and machine learning algorithms to manage energy demand and guarantee the stability of the energy system work effectively. Lyu et al. [14] developed a comprehensive model that deeply analyzed the seasonality of new energy production capacity, the volatility of energy load, and the economic factors of pricing and dispatch to create an

Manuscript received September 1, 2023; revised January 17, 2024.

This work was supported in part by the Project Supported by National Social Science Fund (19BGL003).

Yi Zhang is a professor of the School of Economics and Management, Shanghai University of Electric Power, Shanghai 200090, China (e-mail: zhangyishxy@163.com).

Lin Li is a postgraduate student of the School of Economics and Management, Shanghai University of Electric Power, Shanghai 200090, China (Corresponding author, phone: +8613120898095; e-mail: llin3651@163.com).

Wei Hu is a professor of the School of Economics and Management, Shanghai University of Electric Power, Shanghai 200090, China (e-mail: hwshiep@shiep.edu.cn).

integrated demand response model for thermoelectric power and a stable dispatch model for the vehicle network. The above literature focuses on how end-users respond to demand response, but neglects the interactions between the energy production and utilization side of the equation.

To further optimize the integrated energy utilization mode and tap into the regulating capabilities of energy providers and users, the new concept of integrated energy demand response was first introduced by Sheikhi et al. [15]. The core idea is that the energy supply side leverages the complementary and transformative connection among various energy sources to increase the adaptability of demand response. This is achieved by modifying the type and timing of energy consumption, to fulfill users' requirements for diverse energy applications, including electric, thermal, and cooling loads. The application of integrated energy demand response in load optimization scheduling has been studied by some scholars, mostly from the perspective of game theory and optimization decision methods. For example, Pan et al. [16] constructed an integrated efficiency optimization model including multiple energy forms to explore the optimal mode of system operation, aiming to seek to realize the maximum economic, environmental and energy benefits. Li et al. [17] introduced a game model including several subjects, including energy merchants, suppliers, and end-users, and employed a distributed algorithm that combined quadratic programming and genetic algorithms to achieve optimal outcomes. Cheng et al. [18] develop a model of an N-population asymmetric evolutionary game using replicator dynamics from evolutionary game theory, which aims to offer direction for decision-making by imperfectly rational individuals. Li et al. [19] establish an integrated demand response model containing multiple load types and propose a one-master-multi-slave interactive equilibrium model. Cui et al. [20] focused on the issue of low carbon capture levels in thermal power units throughout the low-carbon transformation process and provided an IES dispatch model that integrates power and heating demand response strategies to enhance the environmental friendliness of IES. Wu et al. [21] designed a bi-level energy trading model covering integrated energy service providers and customers, in which the main objective of the top tier is to increase the profitability of comprehensive energy service providers, while the main task of the bottom tier is to scale down the costs incurred by users. Wang et al. [22] propose a power plant operation optimization model that introduces a hierarchical carbon trading mechanism, aiming to thoroughly study the impact of demand response on carbon emission reduction.

In summary, at present, in the research field of IES integrated demand response, most scholars primarily focus on analyzing the optimal scheduling problem on energy source providers or end-users based on a single energy type. In addition, they do not fully consider the cost implications of exceeding or falling below the carbon emission quota. Therefore, this paper proposes an integrated energy demand response model considering supply-demand synergy and the reward and punishment stepped carbon trading mechanism, and sets up four scenarios to validate the model with integrated energy demand response and carbon trading mechanism as variables.

The findings illustrate the model of this paper accurately describes the process of energy transfer, leverages the mutually beneficial connection among various energy sources within the system, and improves the system's financial feasibility and resilience against disturbances. Additionally, the model achieves energy savings, carbon reduction, and improves the defense, resilience and adaptability of the system.

II. Operation Architecture of Integrated Energy System

Integrated Energy System (IES) has three primary components: the energy supply side, the coupling conversion side, and the terminal demand side. The IES operational architecture has been visualized in Figure 1 [23]-[24].

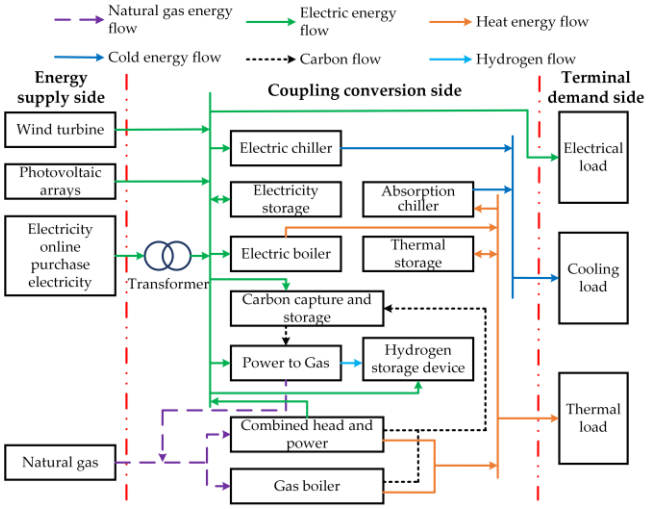

Fig. 1. IES operational architecture.

A. Energy Supply Side

The energy supply for the IES is mainly from wind turbines (WT), photovoltaic arrays (PV), purchased electrical energy from the grid, and purchased natural gas, which is converted into loads required by the system through coupled conversion equipment to meet the system's working requirements [25]. Photovoltaic and wind power generation are characterized by safety, reliability and low generation costs, and the electric load they provide helps to alleviate the pressure on power purchases in IES. Photovoltaic and wind power are respectively affected by light intensity and wind speed, and their output loads are denoted as:

$$P_{PV}^{e}(t) = S_{PV}\eta_{PV}\varphi_{sun}(t) \tag{1}$$

$$P_{WT}^{e}(t) = \begin{cases} 0, v(t) < v_i; v(t) > v_o \\ \dfrac{v(t) - v_i}{v_s - v_i} P_s, v_i \le v(t) \le v_s \\ P_s, v_s < v(t) \le v_o \end{cases} \tag{2}$$

Where $P_{PV}^{e}(t)$ denotes the electrical load output by the PV at period t; S_{PV} and η_{PV} are the light area and light-to-power efficiency of the PV; $\varphi_{sun}(t)$ represent the light intensity at period t; $P_{WT}^{e}(t)$ and $v(t)$ represent the output electrical load of WT and actual wind speed at period t; P_s, v_i, v_s and v_o

are the rated power, cut-in wind speed, rated wind speed, and cut-out wind speed of WT.

B. Coupling Conversion Side

The coupling conversion side serves as the focal point for converting loads in the IES, enabling the efficient conversion of electrical, thermal and cooling loads by leveraging the interdependent link between equipment. The rationale of the conversion method is to enhance the defensiveness and toughness of the IES, and end-users can actively adjust or decrease the power demand during periods of high demand, to guarantee the efficient and smooth work of the electricity system [26].

①Transformer

When electrical energy bought from outside the grid is input into the transformer, a certain amount of power loss occurs and the amount of power it produces is calculated as:

$$P_T^e(t) = \left(1-\eta_T^e\right) P_{buy}^e(t) \tag{3}$$

Where $P_T^e(t)$ denotes the electrical load output from the transformer (T) at time *t*; η_T^e denotes the electrical load loss rate of the T; $P_{buy}^e(t)$ denotes the grid purchased load at time *t*.

②Electric Chiller and Absorption Chiller

Electric chiller (EC) devices cool by consuming electrical loads, absorption chiller (AC) uses the vaporization and heat absorption effect of liquid refrigerant to cool, and the formulas for calculating their output power are denoted as:

$$\begin{cases} P_{EC}^c(t) = \eta_{EC} P_{EC}^e(t) \\ P_{AC}^c(t) = \eta_{AC} P_{AC}^h(t) \end{cases} \tag{4}$$

Where $P_{EC}^c(t)$ and $P_{AC}^c(t)$ represent the cooling load output by EC and AC at period *t*; η_{EC} and η_{AC} represent the refrigeration performance coefficients of EC and AC; $P_{EC}^e(t)$ and $P_{AC}^h(t)$ represent the input electric load and thermal load of EC and AC at time *t*.

③Combined Head and Power and Gas Boiler

Combined heat and power (CHP) uses waste thermal recovery systems to provide heat throughout gas-fired power production, and when the heat supply is inadequate, the gas boiler (GB) supplements the thermal energy by firing natural gas [27]. The formulas for calculating the output of CHP and GB are denoted as:

$$\begin{cases} P_{CHP}^e(t) = G_{ng}^{CHP}(t) L_{ng} \eta_{CHP}^e \\ P_{CHP}^h(t) = G_{ng}^{CHP}(t) L_{ng} \eta_{CHP}^h \\ P_{GB}^h(t) = G_{ng}^{GB}(t) L_{ng} \eta_{GB}^h \end{cases} \tag{5}$$

Where $P_{CHP}^e(t)$ and $P_{CHP}^h(t)$ represent the output electric and heat loads by CHP in period *t*; $G_{ng}^{CHP}(t)$ and $G_{ng}^{GB}(t)$ denote the usage of natural gas during time *t* for CHP and GB; η_{CHP}^e and η_{CHP}^h represent the gas-to-electricity and gas-to-heat efficiencies of CHP; $P_{GB}^h(t)$ denotes the thermal load output of the GB in period *t*; η_{GB}^h denotes the efficiency of gas to heat transfer from GB; L_{ng} denotes the calorific capacity of natural gas, taken as $9.7kWh/m^3$.

④Electric Boiler

The electric boiler (EB) is connected to the heat network and converts the electrical load of the unit into thermal load, the formula for calculating the output power is denoted as:

$$P_{EB}^h(t) = \eta_{EB} P_{EB}^e(t) \tag{6}$$

Where η_{EB} represents the heat production rate of EB; $P_{EB}^h(t)$ and $P_{EB}^e(t)$ denote the thermal load output and electric load input of EB at period *t*.

⑤Carbon Capture and Storage and Power to Gas

By combining carbon capture and storage (CCS) with power to gas (P2G) in IES, the CCS will capture and store some of the carbon generated by CHP and GB, and transport the other part of the carbon as methane raw materials to the P2G [28]. Since the system needs to be low-carbon and low-cost to operate, the P2G breaks down and transforms electric loads into natural gas when the combined working expenses of P2G are below the expenses of purchased electricity, the conversion process has been visualized in Figure 2.

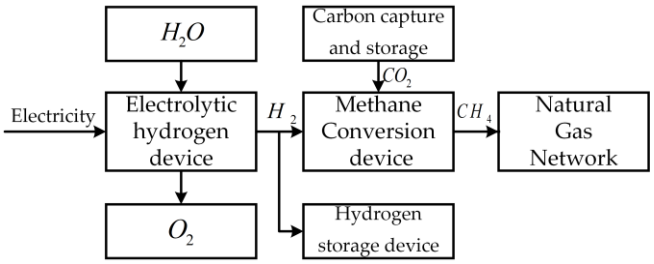

Fig. 2. Schematic diagram of the process of converting electricity to natural gas.

The chemical equation is:

$$2H_2O \xrightarrow{\text{energize}} 2H_2 + O_2 \tag{7}$$

$$CO_2 + 4H_2 \xrightarrow[\text{high temperature}]{\text{high pressure}} CH_4 + 2H_2O \tag{8}$$

The joint operation procedure is represented as:

$$\begin{cases} P_{CCS}^e(t) = P_{CCSF}^e(t) + P_{CCSM}^e(t) \\ P_{CCSM}^e(t) = \eta_{CCS}^C G_{CCS}^C(t) \\ G_{CCS}^C(t) = \eta_{CHP}^C G_{CHP}^C(t) + \eta_{GB}^C G_{GB}^C(t) \\ G_{CHP}^C(t) = \lambda_{CHP}^C [P_{CHP}^e(t) + P_{CHP}^h(t)] \\ G_{GB}^C(t) = \lambda_{GB}^C P_{GB}^h(t) \\ G_{CCS}^{CF}(t) = \eta_{CCS}^{CF} G_{CCS}^C(t) \\ G_{CCS}^{CY}(t) = \eta_{CCS}^{CY} G_{CCS}^C(t) \\ \eta_{CCS}^{CF} + \eta_{CCS}^{CY} = 1 \\ V_{P2G}^{CH_4}(t) = \eta_{CH_4} G_{CCS}^{CY}(t) \\ P_{P2G}^e(t) = V_{P2G}^{CH_4}(t) / \eta_{P2G}^{CH_4} \\ G_{P2G}^{CO_2}(t) = \alpha V_{P2G}^{CH_4}(t) \end{cases} \tag{9}$$

Where $P_{CCS}^e(t)$ denotes the electricity used by CCS in period *t*; $P_{CCSF}^e(t)$ and $P_{CCSM}^e(t)$ denote the fixed and running electricity

consumed by CCS in period *t*; η_{CCS}^{C} denotes the electric power generated by the CCS treatment unit of carbon dioxide; $G_{CCS}^{C}(t)$ is the total amount of CO_2 captured by CCS at time *t*; η_{CHP}^{C} and η_{GB}^{C} denote the carbon capture rates of CHP and GB; $G_{CHP}^{C}(t)$ and $G_{GB}^{C}(t)$ represent the amount of CO_2 produced by CHP and GB in period *t*; λ_{CHP}^{C} and λ_{GB}^{C} denote the carbon intensity when CHP and GB produce one unit of energy respectively; $G_{CCS}^{CF}(t)$ and $G_{CCS}^{CY}(t)$ are carbon emissions stored by CCS and delivered to P2G in time period *t*; η_{CCS}^{CF} and η_{CCS}^{CY} are the proportion of carbon emissions sequestered and delivered to P2G by CHP; $V_{P2G}^{CH_4}(t)$ and $G_{P2G}^{CO_2}(t)$ are the amount of methane produced and CO_2 absorbed in period *t* by P2G; η_{CH_4} denotes the efficiency of electro-gas conversion for P2G; $P_{P2G}^{e}(t)$ represents the electric load consumed by P2G in period *t*; $\eta_{P2G}^{CH_4}$ and α denote the rate of methanation and CO_2 absorption factor of the P2G.

⑥Energy Storage Devices

Energy storage devices respond positively to load-optimized scheduling in IES through low-valley storage and peak supply mechanisms [29]. The energy transfer methods of electric storage (ES), thermal storage (TS), and hydrogen storage device (HSD) are similar, so this paper adopts a unified model representation, and their stored energy be calculated as below:

$$\begin{cases} P_x(t) = (1-\alpha_x)P_x(t-1) + b_x^{chr}(t)\eta_x^{chr}P_x^{chr}(t)\Delta t \\ \qquad -b_x^{dis}(t)P_x^{dis}(t)\Delta t / \eta_x^{dis} \\ 0 \le b_x^{chr}(t) + b_x^{dis}(t) \le 1 \end{cases} \tag{10}$$

Where: x represents each energy storage device, indicating ES, TS, and HSD; $b_x^{chr}(t)$ and $b_x^{dis}(t)$ denote 0-1 variables, when $b_x^{chr}(t)=1$, it represents the energy storage device stores energy at period *t*, otherwise $b_x^{chr}(t)=0$; when $b_x^{dis}(t)=1$, it represents the energy storage device provides energy at period *t*, otherwise $b_x^{dis}(t)=0$; α_x, η_x^{chr} and η_x^{dis} are the self-loss rate, energy storage efficiency and energy supply efficiency of energy storage equipment; $P_x^{chr}(t)$ and $P_x^{dis}(t)$ represent the stored and supplied energy power by energy storage devices at time *t*; $P_x(t)$ and $P_x(t-1)$ represent the amount of energy stored in the energy storage devices at periods *t* and $t-1$.

C. Terminal Demand Side

The terminal demand side provides efficient, environmentally friendly, and economical energy services to customers by aggregating the loads formed on the coupling conversion side to achieve a flexible supply of loads. Among them, wind turbine, photovoltaic arrays, online electricity, ES and CHP supply electrical load to users; electric chiller and absorption chiller supply cooling load to users; and EB, TS, CHP and GB supply thermal load to users.

III. Carbon Trading Mechanism

The core implication of the carbon trading mechanism is to regard carbon emission quotas as tradable commodities. The implementation of trading quotas through the carbon trading platform can incentivize enterprises to actively participate in energy conservation and emission control, thereby progressively attaining the objective of environmentally friendly and low-carbon development.

A. Initial Carbon Emission Allowance Calculation

The main methods currently used in China for the initial allocation of carbon quotas are free quotas and paid quotas [30]. To actively respond to the national energy conservation and emission reduction policy, this paper chooses the free quota allocation method and considers all electricity bought out of the grid as coal-fired thermal generation. Therefore, the carbon emissions in IES are primarily from electricity bought from the grid, CHP, and GB, which are calculated as below:

$$\begin{cases} E_{IES}^{*} = E_{buy}^{*} + E_{CHP}^{*} + E_{GB}^{*} \\ E_{buy}^{*} = \gamma_e \sum_{t=1}^{T} P_{buy}^{e}(t) \\ E_{CHP}^{*} = \gamma_e \sum_{t=1}^{T} P_{CHP}^{e}(t) + \gamma_h \sum_{t=1}^{T} P_{CHP}^{h}(t) \\ E_{GB}^{*} = \gamma_h \sum_{t=1}^{T} P_{GB}^{h}(t) \end{cases} \tag{11}$$

Where E_{IES}^{*}, E_{buy}^{*}, E_{CHP}^{*} and E_{GB}^{*} denote carbon emission quotas allocated to IES, electricity bought out of the grid, CHP and GB; γ_e, γ_h denote the free carbon emission quotas for generating one unit of electricity and heat; T is a demand response cycle.

B. Actual Carbon Emission Calculation

Since the P2G consumes a portion of CO_2 during hydrogen methanation and the CCS sequesters a portion of CO_2 while operating, the IES actual carbon emission is calculated as:

$$\begin{cases} E_{IES} = E_{buy} + E_{CHP} + E_{GB} - E_{P2G} - E_{CCS} \\ E_{buy} = \gamma_e \sum_{t=1}^{T} P_{buy}^{e}(t) \\ E_{CHP} = \gamma_e \sum_{t=1}^{T} P_{CHP}^{e}(t) + \gamma_h \sum_{t=1}^{T} P_{CHP}^{h}(t) \\ E_{GB} = \gamma_h \sum_{t=1}^{T} P_{GB}^{h}(t) \\ E_{P2G} = \sum_{t=1}^{T} G_{P2G}^{CO_2}(t) \\ E_{CCS} = \sum_{t=1}^{T} G_{CCS}^{C}(t) \end{cases} \tag{12}$$

Where E_{IES}, E_{buy}, E_{CHP} and E_{GB} denote the real CO_2 emissions of IES, electricity bought out of the grid, CHP, and GB; E_{P2G} denote the amount of CO_2 taken up by P2G; E_{CCS} refers to the amount of CO_2 stored by CCS.

C. Reward and Punishment Stepped Carbon Trading

Aiming at the green operation of IES, this paper constructs a reward and punishment stepped carbon trading model. If the allocated carbon allowance of IES exceeds the real carbon emissions, the energy supply business has the option to sell the excess credits for economic gain; conversely, the business buys the quotas. The reward and punishment stepped carbon trading model is:

$$C_{CO_2}=\begin{cases}-c(1+\mu_r)k-c(1+2\mu_r)\left(E^*_{IES}-k-E_{IES}\right)\\ ,E_{IES}\le E^*_{IES}-k\\ -c(1+\mu_r)\left(E^*_{IES}-E_{IES}\right)\\ ,E^*_{IES}-k<E_{IES}\le E^*_{IES}\\ c\left(E_{IES}-E^*_{IES}\right)\\ ,E^*_{IES}<E_{IES}\le E^*_{IES}+k\\ ck+c(1+\mu_p)\left(E_{IES}-E^*_{IES}-k\right)\\ ,E^*_{IES}+k<E_{IES}\le E^*_{IES}+2k\\ c(2+\mu_p)k+c(1+2\mu_p)\left(E_{IES}-E^*_{IES}-2k\right)\\ ,E^*_{IES}+2k<E_{IES}\le E^*_{IES}+3k\\ c(3+3\mu_p)k+c(1+3\mu_p)\left(E_{IES}-E^*_{IES}-3k\right)\\ ,E_{IES}>E^*_{IES}+3k\end{cases} \tag{13}$$

Where c denotes baseline pricing for carbon emissions trading; μ_r and μ_p are the reward and punishment factors for different carbon emission intervals; k is the stepped carbon emission interval length; C_{CO_2} denotes the stepped carbon trading cost in IES.

IV. Optimization Scheduling Model for Integrated Energy Demand Response

An integrated energy system operating architecture effectively demonstrates the link between energy transformations inside the IES. On this basis, by structuring the integrated demand response optimization scheduling model, the energy allocation effect is improved and the overall operation cost is minimized under the conditions of meeting the power balance, carbon sequestration and end-user energy demand constraints.

A. Objective Function

The objective function of this paper consists of the minimum of the total operation cost C_{total} in a scheduling cycle, including energy purchase cost C_{buy}, compensation for implementing demand response C_{bc}, carbon trading cost C_{CO_2}, and equipment maintenance cost C_m, namely:

$$\min C_{total}=\min\left(C_{buy}-C_{bc}+C_{CO_2}+C_m\right) \tag{14}$$

①Energy Purchase Cost

The energy procurement expenses of IES primarily consist of three parts: the power procurement expenses from the power grid, the expenses associated with purchasing natural gas for CHP, and the expenses related to purchasing natural gas for GB. Therefore, the total energy purchase cost is:

$$\begin{aligned}C_{buy}=&\sum_{t=1}^{T}\gamma_e^C(t)P_{buy}^e(t)\\&+\sum_{t=1}^{T}\gamma_{ng}^C(t)\left[G_{ng}^{CHP}(t)+G_{ng}^{GB}(t)\right]\end{aligned} \tag{15}$$

Where $\gamma_e^C(t)$ and $\gamma_{ng}^C(t)$ represent the prices of purchasing power and natural gas in period *t*.

②Compensation for Implementing Demand Response

In IES, users' spontaneous participation in demand response both optimizes the energy usage pattern and obtains certain compensation costs. The compensation calculation expression for user implementation of demand response is:

$$\begin{cases}C_{bc}=\sum_{t=1}^{T}\sum_{y=1}^{3}\left[\gamma_{re}^y\left(P_{DR\_B}^y(t)-P_{DR}^y(t)\right)b_{DR}^y(t)\right]\\ P_{DR}^y(t)=P_{DR\_B}^y(t)+P_{tr\_in}^y(t)-P_{tr\_out}^y(t)-P_{re}^y(t)\\ b_{DR}^y(t)=\begin{cases}1,P_{DR\_B}^y(t)-P_{DR}^y(t)>0\\0,P_{DR\_B}^y(t)-P_{DR}^y(t)\le 0\end{cases}\end{cases} \tag{16}$$

Where y represents the type of energy, which is electrical energy (e), heat energy (h), and cold energy (c); γ_{re}^y is the compensation cost per unit load reduction for the $y-th$ energy source; $P_{tr\_in}^y(t)$, $P_{tr\_out}^y(t)$ and $P_{re}^y(t)$ denote the $y-th$ energy transfer in, transfer out and load shedding at time period *t*; $b_{DR}^y(t)$ indicates that if the real load of the $y-th$ energy source in period *t* is lower than the original load, it takes the value of 1; on the contrary, the value is 0; $P_{DR\_B}^y(t)$ and $P_{DR}^y(t)$ represent the loads before and after the $y-th$ energy source engages in demand response in period *t*.

③Equipment Maintenance Cost

During the actual operation of IES, the maintenance of coupling conversion side equipment will incur equipment maintenance costs, namely:

$$C_m=\sum_{t=1}^{T}\left\{\begin{aligned}&c_{EC}^mP_{EC}^c(t)+c_{EB}^mP_{EB}^h(t)\\&+c_{CHP}^m\left[P_{CHP}^e(t)+P_{CHP}^h(t)\right]\\&+c_{GB}^mP_{GB}^h(t)+c_{AC}^mP_{AC}^c(t)\\&+c_{P2G}^mP_{P2G}^e(t)+c_{CCS}^mP_{CCS}^e(t)\\&+c_T^mP_T^e(t)+\sum_{x=1}^{3}\left[c_x^mP_x(t)\right]\end{aligned}\right\} \tag{17}$$

Where c_{EC}^m, c_{EB}^m, c_{CHP}^m, c_{GB}^m, c_{AC}^m, c_{P2G}^m, c_{CCS}^m and c_T^m are the equipment maintenance costs per unit of energy production for EC, EB, CHP, GB, AC, P2G, CCS, and T; c_x^m is the equipment maintenance cost per unit of stored energy for the x-th type of energy storage devices.

B. Constraints

①Power Balance

The power balance constraint indicates that a balanced relationship is maintained between the amount of energy supplied and energy demanded at any time during the demand

response cycle. This constraint contains the power balance of electrical, thermal, and cooling energy expressed as:

$$\begin{cases} P_{PV}^{e}(t)+P_{WT}^{e}(t)+P_{T}^{e}(t)+P_{CHP}^{e}(t)+P_{es}^{dis}(t)= \\ P_{EC}^{e}(t)+P_{EB}^{e}(t)+P_{CCS}^{e}(t)+P_{P2G}^{e}(t)+P_{es}^{chr}(t)+P_{DR}^{e}(t) \\ P_{EB}^{h}(t)+P_{CHP}^{h}(t)+P_{GB}^{h}(t)+P_{ts}^{dis}(t)= \\ P_{AC}^{h}(t)+P_{ts}^{chr}(t)+P_{DR}^{h}(t) \\ P_{EC}^{c}(t)+P_{AC}^{c}(t)=P_{DR}^{c}(t) \end{cases} \tag{18}$$

②Energy Storage Devices

At any time in the demand response cycle, the storage carrying capacity of the energy storage device varies with energy dispatch, and the following constraints require being fulfilled:

$$\begin{cases} 0 \le P_{x}(t) \le P_{x}^{\max} \\ 0 \le P_{x}^{dis}(t) \le P_{x\max}^{dis} \\ 0 \le P_{x}^{chr}(t) \le P_{x\max}^{chr} \end{cases} \tag{19}$$

Where: $P_{x}^{\max}$, $P_{x\max}^{chr}$ and $P_{x\max}^{dis}$ are the maximum energy storage capacity, the largest energy storage power, and the largest energy supply power of the energy storage device.

③Energy Conversion Devices Operating

Each energy conversion equipment has load constraints during operation and requires the following conditions to be met:

$$\begin{cases} P_{EC\_\min}^{e} \le P_{EC}^{e}(t) \le P_{EC\_\max}^{e} \\ P_{EB\_\min}^{e} \le P_{EB}^{e}(t) \le P_{EB\_\max}^{e} \\ P_{AC\_\min}^{h} \le P_{AC}^{h}(t) \le P_{AC\_\max}^{h} \\ P_{CHP\_\min}^{e} \le P_{CHP}^{e}(t) \le P_{CHP\_\max}^{e} \\ P_{CHP\_\min}^{h} \le P_{CHP}^{h}(t) \le P_{CHP\_\max}^{h} \\ P_{GB\_\min}^{h} \le P_{GB}^{h}(t) \le P_{GB\_\max}^{h} \\ P_{CCS\_\min}^{e} \le P_{CCS}^{e}(t) \le P_{CCS\_\max}^{e} \\ P_{P2G\_\min}^{e} \le P_{P2G}^{e}(t) \le P_{P2G\_\max}^{e} \end{cases} \tag{20}$$

Where $P_{EC\_\min}^{e}$ and $P_{EC\_\max}^{e}$ denote the lowest and highest amounts of electrical loads per unit time input to the EC; $P_{EB\_\min}^{e}$ and $P_{EB\_\max}^{e}$ represent the lowest and highest electrical loads input per unit time of the EB; $P_{AC\_\min}^{h}$ and $P_{AC\_\max}^{h}$ represent the lowest and highest thermal load per unit time input to the AC; $P_{CHP\_\min}^{e}$ and $P_{CHP\_\max}^{e}$ represent the lowest and highest electrical load output per unit time for CHP; $P_{CHP\_\min}^{h}$ and $P_{CHP\_\max}^{h}$ denote the lowest and highest thermal load output per unit time for CHP; $P_{GB\_\min}^{h}$ and $P_{GB\_\max}^{h}$ represent the lowest and highest thermal load per unit time output of the GB; $P_{CCS\_\min}^{e}$ and $P_{CCS\_\max}^{e}$ denote the lowest and highest electrical loads per unit time input to the CCS; $P_{P2G\_\min}^{e}$ and $P_{P2G\_\max}^{e}$ denote the lowest and highest electrical loads per unit time input of the P2G.

④Demand Response Load

Transferable load pertains to the ability of electricity consumers to decrease or delay the amount of electricity needed during peak hours, without impacting the overall electricity demand of the IES throughout the dispatching cycle. The constraints to be fulfilled by the transferable load amount are:

$$\begin{cases} \sum_{t=1}^{T} P_{tr\_out}^{y}(t) = \sum_{t=1}^{T} P_{tr\_in}^{y}(t) \\ 0 \le P_{tr\_in}^{y}(t) \le b_{tr\_in}^{y}(t)\delta_{tr}^{y}P_{DR\_B}^{y}(t) \\ 0 \le P_{tr\_out}^{y}(t) \le b_{tr\_out}^{y}(t)\delta_{tr}^{y}P_{DR\_B}^{y}(t) \\ 0 \le b_{tr\_in}^{y}(t)+b_{tr\_out}^{y}(t) \le 1 \end{cases} \tag{21}$$

Where δ_{tr}^{y} is the proportion of the load allowed to be shifted by the *y-th* energy in the load before demand response, and the value is 5% ; Both $b_{tr\_in}^{y}(t)$ and $b_{tr\_out}^{y}(t)$ are $0-1$ variables, and the values of 1 indicate that the *y-th* energy source is in the turn-in and turn-out states in period *t*; on the contrary, the value is 0.

Reducible load means that users can reduce part of power demand independently without affecting normal electricity consumption. The constraint that the reducible load is required to satisfy is:

$$0 \le P_{re}^{y}(t) \le \delta_{re}P_{DR\_B}^{y}(t) \tag{22}$$

Where δ_{re}^{y} is the proportion of the reducible load by the *y-th* energy source to the pre-demand response load, and takes the value of 5%.

⑤Energy Satisfaction

When guiding end users to change their energy consumption habits, it is necessary to consider their satisfaction with energy consumption. The more users adjust their electricity demand, the lower their satisfaction with energy consumption. Energy satisfaction constraints need to meet the following constraints:

$$\begin{cases} \rho_{s} = \frac{1}{3}\sum_{y=1}^{3}\left\{\frac{1}{T}\sum_{t=1}^{T}\left[1-\frac{\left|P_{DR}^{y}(t)-P_{DR\_B}^{y}(t)\right|}{P_{DR\_B}^{y}(t)}\right]\right\} \\ \rho_{s\min} \le \rho_{s} \le 1 \end{cases} \tag{23}$$

Where ρ_{s} and $\rho_{s\min}$ are the user satisfaction level and the minimum user satisfaction level.

⑥Carbon Sequestration

Due to the leakage risk of excessive CO_2 storage, the following constraints are required to be met for carbon sequestration by CCS:

$$0 \le G_{CCS}^{C}(t) \le G_{CCS\_\max}^{C} \tag{24}$$

Where: $G_{CCS\_\max}^{C}$ denotes the peak value of CO_2 storage capacity of CCS.

V. Case Study

A. Input Data

To validate the environmental friendliness and effectiveness of the proposed integrated energy demand response optimization scheduling model, this paper conducts a case study of a park IES containing electricity, thermal, and cold energy. Set the IES single day 24h as an optimized

scheduling cycle with a step size of 1h. Initial demand of electrical, thermal and cooling loads at the end of the system as shown in Figure 3. The WT and PV predicted output power is illustrated in Figure 4. Grid tariff, Time-sharing tariffs and time-sharing gas tariffs are illustrated in Figure 5. The parameters of the coupling conversion side equipment in the system are shown in Table I. The parameters of the energy storage devices are presented in Table II.

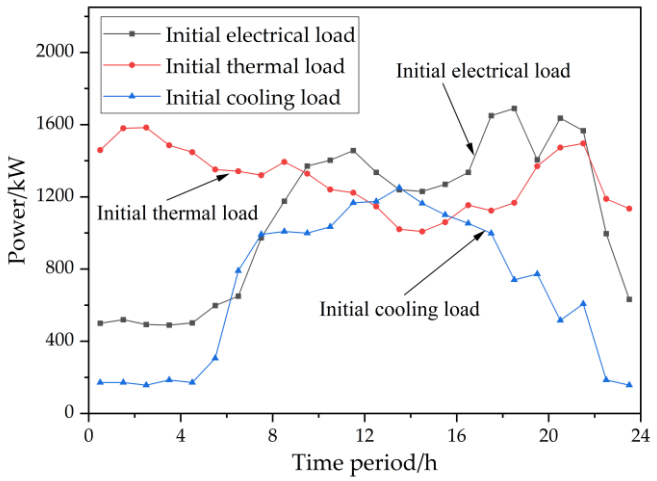

Fig. 3. Initial demand of electrical, thermal and cooling loads at the end of the system.

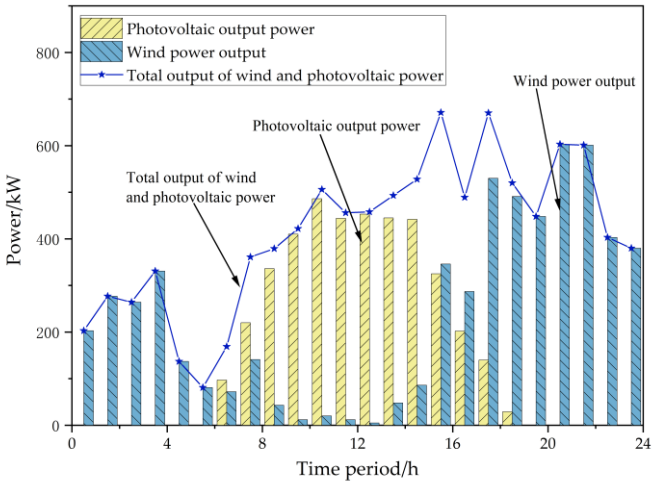

Fig. 4. Wind and photovoltaic predicted output.

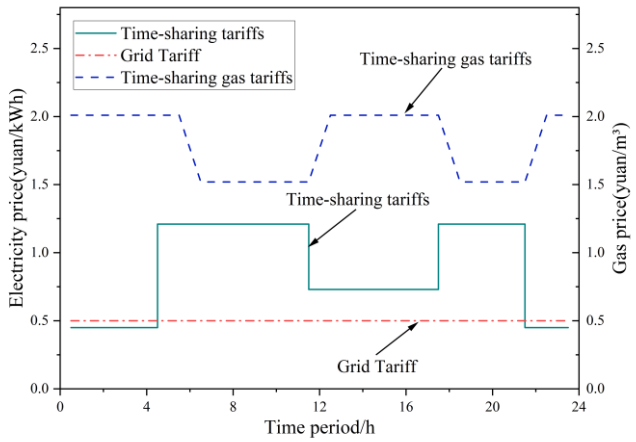

Fig. 5. Grid tariff, time-sharing tariffs and time-sharing gas tariffs.

When implementing the comprehensive demand response, the compensation costs for the reduction of unit electrical load, thermal load and cooling load are 0.3(yuan/kW · h), 0.2(yuan/kW · h) and 0.2(yuan/kW · h). The basic price of carbon trading is 400yuan/t. The stepped carbon emission interval length is 1t. The reward and punishment factors for different carbon emission intervals are 0.2 and 0.3.

This paper presents a load optimization scheduling model, which is a mixed integer linear programming model (the objective function is (14) and the constraints are (18)-(24)), and the algorithm is modeled and solved based on the Matlab platform using the YALMIP toolbox and the CPLEX Solver.

TABLE I
PARAMETERS OF COUPLING CONVERSION SIDE EQUIPMENT WITHIN THE INTEGRATED ENERGY SYSTEM

Equipment Name	Equipment Parameters
EC	$\eta_{EC}=4, c^{m}_{EC}=0.0114(yuan/kW\cdot h)$, $P^{e}_{EC\_min}=0(kW), P^{e}_{EC\_max}=140(kW)$
EB	$\eta_{EB}=0.9, c^{m}_{EB}=0.0125(yuan/kW\cdot h)$, $P^{e}_{EB\_min}=0(kW), P^{e}_{EB\_max}=100(kW)$
CHP	$P^{e}_{CHP\_min}=0(kW), P^{e}_{CHP\_max}=700(kW)$, $P^{h}_{CHP\_min}=0(kW), P^{h}_{CHP\_max}=500(kW)$, η^{e}_{CHP}=0.35, η^{h}_{CHP}=0.45, c^{m}_{CHP}=0.12$(yuan/kW\cdot h)$,
GB	$\eta^{h}_{GB}=0.9, c^{m}_{GB}=0.18(yuan/kW\cdot h)$, $P^{h}_{GB\_min}=0(kW), P^{h}_{GB\_max}=900(kW)$
AC	η_{AC}=1.2, c^{m}_{AC}=0.016$(yuan/kW\cdot h)$, $P^{h}_{AC\_min}$=0$(kW), P^{h}_{AC_max}=500(kW)$
P2G	η_{CH_4}=0.7, $P^{e}_{P2G\_min}$=0$(kW), P^{e}_{P2G_max}$=150(kW)
CCS	$P^{e}_{CCS\_min}=0(kW), P^{e}_{CCS\_max}=80(kW)$

TABLE II
PARAMETERS OF ENERGY STORAGE DEVICES

Device Parameters	Electricity storage	Heat storage	Hydrogen storage device
α_x	0.01	0.02	0.05
η^{chr}_x	0.90	0.98	0.99
η^{dis}_x	0.90	0.98	0.99
$P^{\max}_x$	500	500	300
$P^{chr}_{x\max}$	300	200	200
$P^{dis}_{x\max}$	200	150	200

B. *Experimental results*

①Experimental Scenarios Setting

To study the impact of carbon trading mechanism and integrated energy demand response on IES load scheduling, this paper establishes four scenarios for comparative analysis, and the details of each scenario can be found in Table III. The 4 scenarios have the same conditions except that the carbon

trading mechanism and whether to implement demand response are different, √ indicates that the condition is considered, × indicates that the condition is not considered, and the traditional carbon trading mechanism is established at 400 (yuan/t).

TABLE III
DIFFERENT SCENARIOS SETTING SITUATION

Scenarios	Traditional Carbon Trading Mechanism	Reward and Punishment Stepped Carbon Trading Mechanism	Integrated energy demand response
Scenario 1	√	×	×
Scenario 2	√	×	√
Scenario 3	×	√	×
Scenario 4	×	√	√

②Optimized Scheduling Results for Each Scenario

According to the integrated energy demand response optimization scheduling model presented in this paper, four scenarios are modeled separately, and the optimization scheduling results for the IES under each scenario are displayed in Table IV. Table IV demonstrates that the implementation of a reward and punishment stepped carbon trading mechanism, along with the consideration of integrated energy demand response, enhances the utilization of energy source integration and conversion.

TABLE IV
IES OPTIMIZED SCHEDULING RESULTS IN DIFFERENT SCENARIOS

Scenarios	Scenario 1	Scenario 2	Scenario 3	Scenario 4
comprehensive operation cost(yuan)	23378.072	20533.610	19860.504	19120.083
Energy Purchase Cost(yuan)	15529.985	17710.782	16787.784	18571.114
Compensation for Implementing Demand Response(yuan)	0.000	-2425.680	0.000	-3017.420
Carbon Trading Cost(yuan)	5128.259	2035.247	504.665	398.731
Equipment Maintenance Cost(yuan)	2719.829	3213.261	2568.055	3167.659
Carbon emissions above allowances(t)	12.821	5.112	1.201	0.997

③Optimized Scheduling Process Analysis for Each Scenario

Scenario 1 does not incorporate the reward and punishment stepped carbon trading mechanism and integrated energy demand response in the optimal scheduling. Instead, it incorporates traditional carbon trading mechanism. The optimized dispatch strategies for electricity, thermal and cooling loads obtained from the analysis are shown in Figure 6, 7, and 8.

As for the electrical load, it mainly comes from the purchase of power by wind turbine, photovoltaic arrays and the grid. The CHP operates at maximum capacity as an additional power supply equipment from 12:00 to 19:00. The IES supplies the necessary power for EC, EB, CCS, and P2G while also meeting the electricity demand. For the thermal load, thermal energy from CHP and GB is much higher than that of EB. The IES not only satisfies the thermal load, but also supplies the necessary thermal energy for the AC. For the cooling load, the IES is more inclined to the EC with strong economy. However, during 6:00-20:00, the EC can not meet the needs of end users, and the AC starts to provide cooling load.

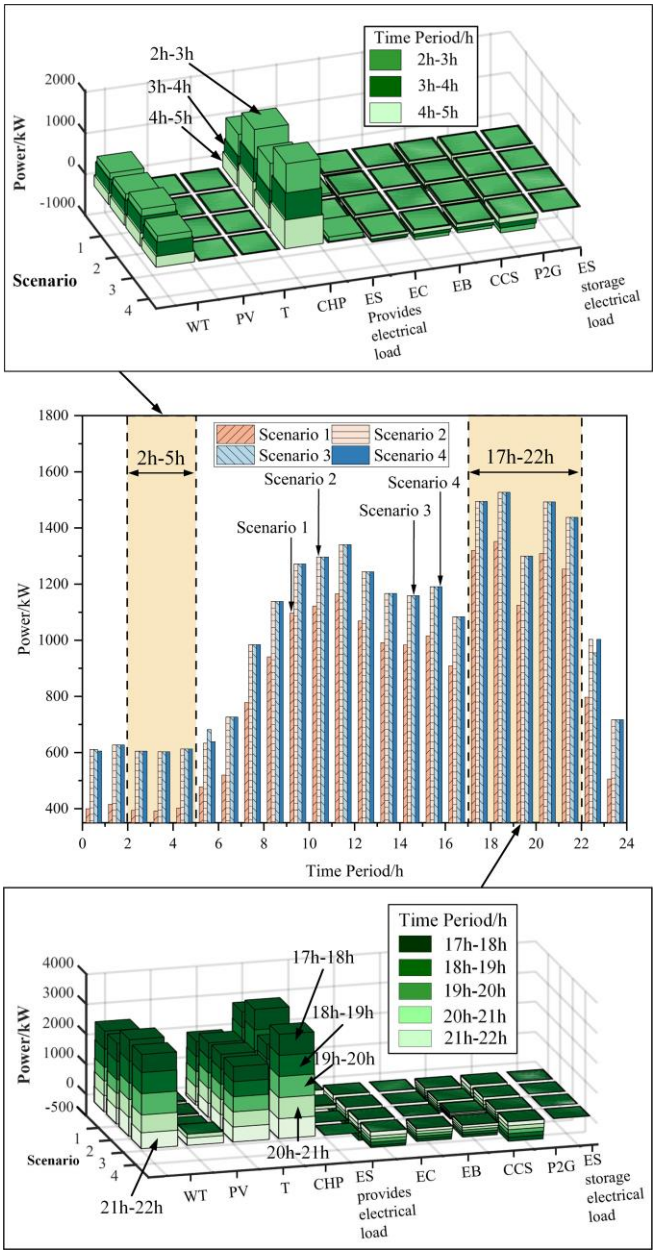

Fig. 6. Electrical load optimization scheduling strategy for four scenarios.

Scenario 2 does not consider the reward and punishment stepped carbon trading mechanism, but considers the integrated energy demand response to participate in the optimal scheduling. The optimal scheduling strategies for electric, heat, and cooling loads are shown in Figures 6, 7, and 8 respectively, and the changes of electric, thermal, and cooling loads before and after the demand response are shown in Figure 9. From the figure, it is concluded that after the end user implemented the comprehensive demand response, the electricity, thermal, and cooling loads changed to a certain extent.

Regarding the electric load, customers reduce the demand for electricity during the high tariff period of 18:00-22:00, and increase the demand for electricity during the low tariff

period of 22:00-5:00 the next day, and this procedure significantly decreases the expense of acquiring energy for IES. Compared to Scenario 1, CHP has increased electrical energy supplied during peak hours and is operating at full capacity most of the time, and the overall load profile is more stable and load volatility is reduced. The user has appropriately shifted the energy and heat demands from 13:00-16:00 to 6:00-13:00 for the thermal load. The heat supply of the CHP is substantially augmented as compared to scenario 1. In contrast, the heat supply of the GB decreases during 0:00-5:00 and 13:00-16:00. Regarding the cooling load, users reduce their requirement for cooling between 5:00 and 18:00 hours. However, the supply of the EC increases dramatically between 20:00 and 5:00 hours of the next day. Additionally, the cooling capacity of the AC is notably reduced between 10:00 and 18:00 hours.

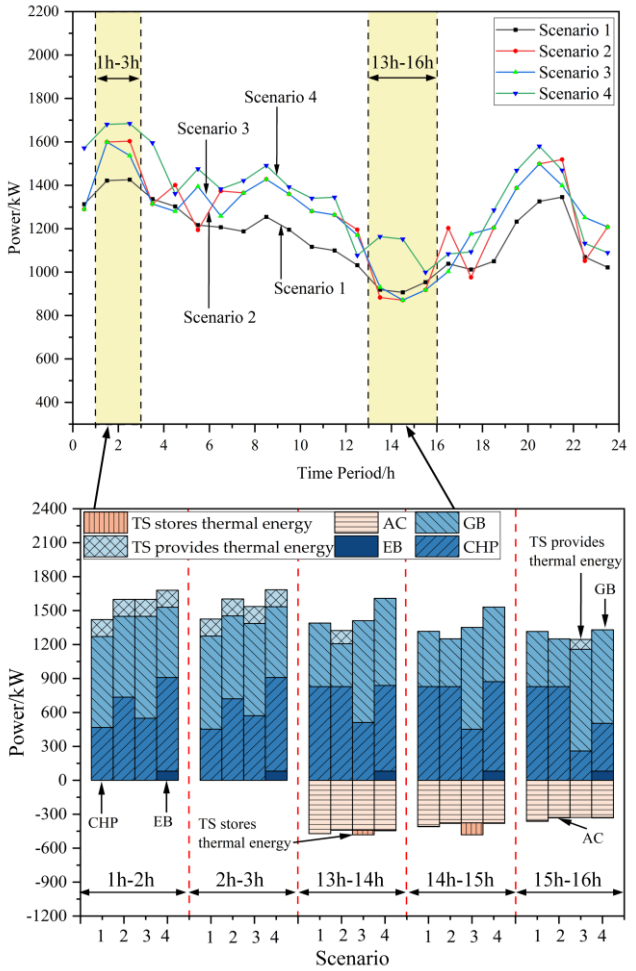

Fig. 7. Thermal load optimization scheduling strategy for four scenarios.

Scenario 3 does not consider the integrated energy demand response, but considers the reward and punishment stepped carbon trading mechanism to be involved in the scheduling. The optimal scheduling strategy for electric, thermal, and cooling loads is shown in Figure 6, 7, and 8. In comparison to scenario 1, excess carbon emission over the quota decreased by 11.619(t), and carbon trading cost decreased by 4623.594(yuan). This suggests that the use of the reward and punishment stepped carbon trading mechanism can effectively enhance the emission reduction benefits in IES compared to the traditional carbon trading mechanism.

Regarding the electrical load, the electric load consumed by CCS declines due to the constraints of the stepped carbon trading mechanism, and the electricity consumed by the P2G has also decreased compared to scenario 1. Regarding the thermal load, the IES favors the CHP and GB for heat delivery, thanks to the cleanliness of natural gas. Therefore, the heat supply in scenario 3 is considerably more than that in scenario 1. For the cooling load, although AC and EC do not consider carbon dioxide emissions, the cooling load also changes due to changes in the demand for electricity and thermal load.

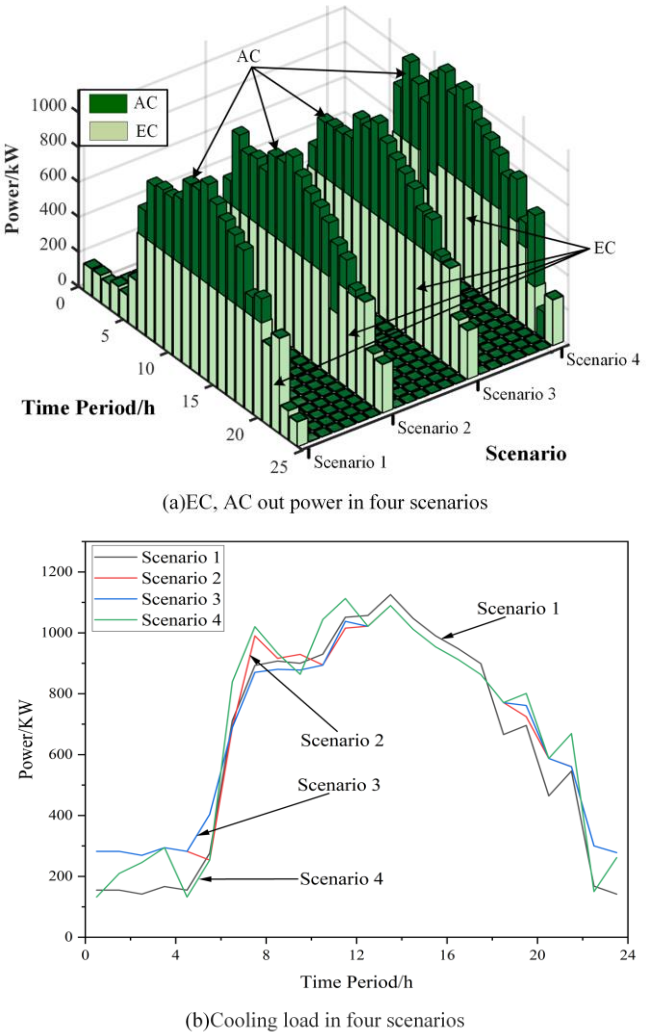

(a)EC, AC out power in four scenarios

(b)Cooling load in four scenarios

Fig. 8. Cooling load optimization scheduling strategy for four scenarios.

Scenario 4 comprehensively considers the reward and punishment stepped carbon trading mechanism and integrated energy demand response. The optimal scheduling strategy of Scenario 4 is more flexible and perfect than the previous three scenarios, and the optimal scheduling strategies for electric, heat, and cooling loads are shown in Figures 6, 7, and 8 respectively, and the changes of electric, thermal, and cooling loads before and after the demand response are shown in Figure 9.

For the electric load, under the effect of integrated energy demand response, IES has greatly reduced the load demand during the 8:00-22:00 high tariff period. Simultaneously, the CHP is operating at maximum capacity to provide power. In case of inadequate power supply, the storage battery can supplement power flexibly, ensuring sufficient power for

standby during peak power consumption. With the introduction of stepped carbon trading mechanism, the electrical load required for CHP and P2G has increased. For the thermal load, the thermal load in IES has been reduced after the implementation of integrated energy demand response, among which: CHP, GB, and EB provide the main heat energy. The HS is utilized as supplementary equipment to provide heat energy promptly during the period from 0:00 to 5:00 when the GB has a heating shortage. In terms of the cooling load, end-users modify their cooling requirements by redistributing their demand from the hours between 8:00 and 18:00 to the hours between 1:00 and 4:00, as well as 18:00 and 22:00. This results in a decrease in the total cooling demand.

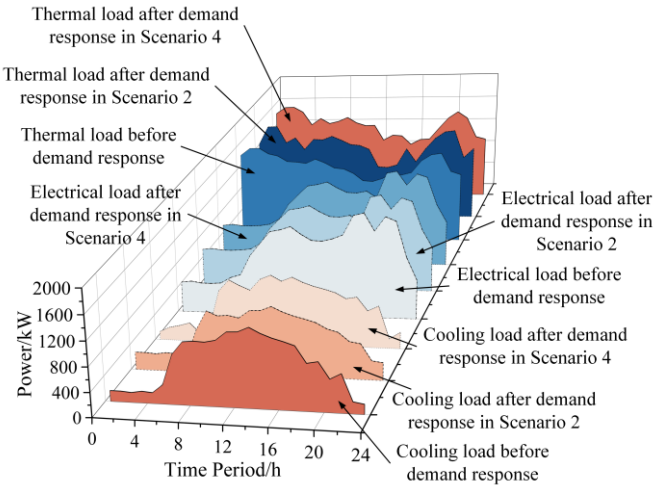

Fig. 9. Scenario 2 and 4 comparison diagram of changes before and after the demand response of electricity, thermal, and cooling loads.

The above-mentioned case analysis demonstrates that by implementing the reward and punishment stepped carbon trading mechanism, along with the integrated energy demand response, IES can flexibly carry out load optimization scheduling according to the time-sharing tariffs, the time-sharing gar tariffs, and energy demand while restricting the carbon emissions of equipment. The optimization strategy of "load reduction + load transfer + energy storage equipment supply" is implemented during high energy consumption periods. Conversely, the "load transfer + energy storage equipment storage" strategy is employed during low energy consumption periods. This approach decreases the demand for power purchased from external sources and maximizes the efficiency of energy distribution and transformation. As a result, it achieves the goals of reducing peak energy demand, filling energy valleys, and promoting energy and carbon savings.

VI. Conclusions

Implementing integrated demand response and carbon trading mechanism is crucial for encouraging energy conservation, lowering carbon emission, and ensuring the efficient running of IES. This paper comprehensively examines the transformable characteristics of electrical, thermal, and cooling loads, constructs an integrated demand response model that considers source-load synergy and reward-punishment stepped carbon trading mechanism, and establishes 4 scenarios for comparison and analysis. The paper draws the following conclusions:

1) The proposed integrated energy demand response optimization scheduling model incorporates different conversion characteristics of different energy devices. This model aims to enhance the efficiency of energy integration and conversion, thereby reducing the strain on equipment supply and improving the capacity of distributed energy consumption. In turn, the model enhances the affordability, and environmental sustainability of system work.
2) Implementing a reward and punishment system for carbon trading can effectively optimize the performance of equipment engaged in the conversion process, resulting in reduced carbon dioxide emissions and trading costs. This, in turn, enhances the system's low-carbon economy.
3) By implementing demand response, it can systematically instruct end users to modify their energy consumption patterns, enabling them to reduce and shift their electricity and gas usage during high electricity and gas prices and peak hours of energy consumption, to effectively decreases the IES's total operating costs.

References

[1] L. Hou, H. J. Lin, X. Yang, T. K. Yang, F. Qu, and D. Shao, "Optimal Scheduling of Integrated Energy Systems for High-speed Railway Stations Considering Integrated Demand Response under the Carbon Market," *IAENG International Journal of Applied Mathematics*, vol. 53, no.2, pp 497-506, 2023

[2] X. P. Ma, Y. Liang, K. Y. Wang, R. Jia, X. Y. Wang, H. D. Du, and H. Liu, "Dispatch for Energy Efficiency Improvement of an Integrated Energy System considering Multiple Types of Low Carbon Factors and Demand Response," *Frontiers In Energy Research*, vol. 10

[3] A. Ghada, A. Abdelfatah, F. S. Mostafa, and E. Essam, "Stochastic multi-objectives optimal scheduling of energy hubs with responsive demands in smart microgrids," *Journal of Energy Storage*, vol. 55, 2022

[4] L. Tian, C. Zhu, and T. Deng, "Day-ahead scheduling of SMR integrated energy system considering heat-electric-cold demand coupling response characteristics," *Energy Reports*, vol. 8, pp13302-13319, 2022

[5] N. Rezaei, Y. Pezhmani, and A. Khazali, "Economic-environmental risk-averse optimal heat and power energy management of a grid-connected multi microgrid system considering demand response and bidding strategy," *Energy*, vol. 240, 2022

[6] P. Subhasis, M. Sarthak, K. Pravat, K. Binod, B. Mohit, M. Hossam, and K. Salah, "Residential Demand Side Management model, optimization and future perspective: A review," *Energy Reports*, vol. 8, pp3727-3766, 2022

[7] P. Yang, H. Jiang, C. Liu, L. Kang, and C. Wang, "Coordinated optimization scheduling operation of integrated energy system considering demand response and carbon trading mechanism," *International Journal of Electrical Power & Energy Systems*, vol. 147, 2023

[8] Q. Xu, Y. Ding, and A. Zheng, "An Optimal Dispatch Model of Wind-Integrated Power System Considering Demand Response and Reliability," *Sustainability*, vol. 9, 2017

[9] Y. Li, J. Wang, Y. Zhang, and Y. Han, "Day-ahead scheduling strategy for integrated heating and power system with high wind power penetration and integrated demand response: A hybrid stochastic/interval approach," *Energy*, vol. 253, 2022

[10] I. Nnamdi, and X. Xia, "Optimal Dispatch for a Microgrid Incorporating Renewables and Demand Response," *Renewable Energy*, vol. 101, pp16-28, 2017

[11] H. Yang, X. Zhang, Y. Ma, and D. Zhang, "Critical peak rebate strategy and application to demand response," *Protection and Control of Modern Power Systems*, vol. 6, pp357-370, 2021

[12] H. Ming, B. Xia, K. Lee, A. Adepoju, S. Shakkottai, and L. Xie, "Prediction and assessment of demand response potential with coupon

incentives in highly renewable power systems," *Protection and Control of Modern Power Systems*, vol. 5, pp124-137, 2020
[13] R. Lu, and S. Hong, "Incentive-based Demand Response for Smart Grid with Reinforcement Learning and Deep Neural Network," *Applied Energy*, vol. 236, pp937-949, 2019
[14] X. Lyu, T. Liu, X. Liu, C. He, L. Nan, and H. Zeng, "Low-carbon Robust Economic Dispatch of Park-level Integrated Energy System Considering Price-based Demand Response and Vehicle-to-grid," *Energy*, vol. 263, 2023
[15] A. Sheikhi, S. Bahrami, and A. Ranjbar, "An Autonomous Demand Response Program for Electricity and Natural Gas Networks in Smart Energy Hubs," *Energy*, vol. 89, pp490-499, 2015
[16] C. Pan, T. Jin, N. Li, G. Wang, X. Hou, and Y. Gu, "Multi-objective and Two-stage Optimization Study of Integrated Energy Systems Considering P2G and Integrated Demand Responses," *Energy*, vol. 270, 2023
[17] K. Li, N. Ye, S. Li, H. Wang, and C. Zhang, "Distributed collaborative operation strategies in multi-agent integrated energy system considering integrated demand response based on game theory," *Energy*, vol. 273, 2023
[18] L. Cheng, R. Yang, G. Liu, J. Wang, Y. Chen, X. Wang, J. Zhang, and T. Yu, "Multi-population Asymmetric Evolutionary Game Dynamics and Its Applications in Power Demand-side Response in Smart Grid," *Proceedings of the Chinese Society of Electrical Engineering*, vol. 40, pp20-36, 2020
[19] P. Li, D. Wu, Y. Li, H. Liu, N. Wang, and X. Zhou, "Optimal Dispatch of Multi-microgrids Integrated Energy System Based on Integrated Demand Response and Stackelberg game," *Proceedings of the Chinese Society of Electrical Engineering*, vol. 41, pp1307-1321, 2021
[20] Y. Cui, C. Gu, X. Fu, G. Deng, Y. Zhao, and Y. Tang, "Low-carbon Economic Dispatch of Integrated Energy System With Carbon Capture Power Plants Considering Generalized Electric Heating Demand Response," *Proceedings of the Chinese Society of Electrical Engineering*, vol. 42, pp8431-8445, 2022
[21] Q. Wu, and C. Li, "Dynamic pricing and energy management of hydrogen-based integrated energy service provider considering integrated demand response with a bi-level approach," *Journal of Energy Storage*, vol. 59, 2023
[22] Y. Wang, Y. Qin, B. Du, Y. Liu, S. Xu, D. Li, and D. Wang, "Operational optimization of an integrated electricity-heat energy system considering demand response under a stepped carbon trading mechanism," *Journal of Physics: Conference Series*, 2022
[23] E. Alizad, H. Rastegar, and F. Hasanzad, "Dynamic planning of Power-to-Gas integrated energy hub considering demand response programs and future market conditions," *International Journal of Electrical Power and Energy Systems*, vol. 143, 2022
[24] H. Jiang, H. Zhou, X. Xie, D. Yang, and Y. Zhao, "Optimal control of integrated energy system considering temperature comfort and carbon trade," *Control Theory and Applications*, vol. 39, pp519-526, 2022
[25] Y. Wang, K. Li, S. Li, X. Ma, and C. Zhang, "A bi-level scheduling strategy for integrated energy systems considering integrated demand response and energy storage co-optimization," *Journal of Energy Storage*, vol. 66, 2023
[26] B. Yu, F. Sun, C. Chen, G. Fu, and L. Hu, "Power demand response in the context of smart home application," *Energy*, vol. 240, 2022
[27] X. Yu, and S. Ergan, "Estimating power demand shaving capacity of buildings on an urban scale using extracted demand response profiles through machine learning models," *Applied Energy*, vol. 310, 2022
[28] M. Iranpour, R. Sadeghi, E. Saghafi, and M. Delshad, "Techno-economic energy management of micro-grid in the presence of distributed generation sources based on demand response programs," *International Journal of Electrical Power and Energy Systems*, vol. 141, 2022
[29] K. Seshu, R. Phani, R. Koteswara, and A. Singh, "Impact of multiple demand side management programs on the optimal operation of grid-connected microgrids," *Applied Energy*, vol. 301, 2021
[30] H. Xiao, F. Long, L. Zeng, W. Zhao, J. Wang, and Y. Li, "Optimal scheduling of regional integrated energy system considering multiple uncertainties and integrated demand response," *Electric Power Systems Research*, vol. 217, 2023

Yi Zhang, male, born in November 1979, Associate Professor, Master Supervisor, graduated from the Department of Electric Power Engineering, Shanghai University of Electric Power, China in July 2001 with a Bachelor's Degree, graduated from the School of Economics and Management, Tongji University, China in March 2010 with a Master's Degree, and is currently studying for a PhD in Management Science and Engineering at the School of Economics and Management, Tongji University, China. He has studied in the Education University of Hong Kong and University of Calgary, Canada. His main research interests are power engineering management, energy system optimization and decision making, and energy blockchain.
He Engaged in teaching and scientific research in the field of power engineering economics and management. He has published more than 10 papers in various academic journals as the first author (including 5 SCI/EI/CSSCI retrievals and 2 Peking University core papers); edited 3 textbooks; presided over or participated in more than 20 projects entrusted by the National Social Science Foundation, the Ministry of Education and energy and power enterprises. He was awarded the first prize of Shanghai Teaching Achievements and Shanghai Yucai Award.